ELSEVIER

Catalysis Today 50 (1999) 207–225

CATALYSIS TODAY

IR study of polycrystalline ceria properties in oxidised and reduced states

Claude Binet, Marco Daturi, Jean-Claude Lavalley*

Laboratoire de Catalyse et Spectrochimie, UMR 6506, URA CNRS 414, ISMRA Universite, 6, Boulevard du Maréchal Juin, 14050, Caen Cedex, France

Abstract

Surface properties of high surface area ceria samples, either in the reduced or unreduced state, have been investigated using FT-IR spectroscopy. Upon reduction, detailed features in the background spectrum of unreduced samples, which may be assigned to surface or multiphonon modes, vanish while weak bands due to electronic transitions appear. One of these bands is assignable to Ce^{3+} as point defect in the core. Adsorption of probe molecules is used to characterise the Lewis acid–base strength of surface sites. Adsorption of a proton donor (pyrrole) or an electronic acceptor (CO_2) is indicative of the high basicity of surface O^{2-} ions for ceria either reduced or not. The acid strength of cerium ions is weak; its decrease upon reduction may be shown by adsorbing weak Lewis bases (CO, acetonitrile) but not by stronger ones (pyridine, dimethylether). Superoxide (O_2^-) or peroxide (O_2^{2-}) surface species are produced when O_2 is adsorbed on surface reduced defects. In the case of samples with a higher degree of reduction, the electron donor power is shown by tetracyanoethylene adsorption. Surface hydroxy and methoxy species from H_2 and methanol dissociations, respectively, are very sensitive probes in differentiating one, two and threefold co-ordinatively unsaturated cationic sites and their reduction state. The use of methoxy species allows to quantify the ceria reduction degree through the addition of known amounts of oxygen. Adsorbed formate species are also sensitive to ceria reduction state.

Keywords: Ceria; IR study; FT-IR spectroscopy

1. Introduction

Ceria has been considered and largely used in the last years as one of the most important promoters of heterogeneous catalytic reactions. For this reason it has been deeply investigated from the scientific and technologic point of view [1].

Ceria (CeO_2) belongs to the fluorite structure. Each O^{2-} anion is surrounded by a tetrahedron of Ce^{4+} cations located at the centre of a cubic arrangement of equivalent O^{2-} atoms. From XPS spectra it was claimed that a mixed-valent ground state of CeO_2 has to be considered due to a partial charge transfer from the filled O 2p orbital (O^{2-}) to the empty $4f^0$ (Ce^{4+}) one [2,3]; this was controvert [4]. Theoretical calculations [5,6] have shown that some covalency takes place between bulk Ce^{4+} and O^{2-} ions. Nevertheless, for simplicity and as done in recent calculations [7,8], CeO_2 is formally considered here as a purely ionic compound constituted of Ce^{4+} and O^{2-} ions, even at the surface. Upon heating CeO_2 at

*Corresponding author. Tel.: +33-31-452814; fax: +33-31-452822; e-mail: lamotte@ismra.unicaen.fr

0920-5861/99/$ – see front matter
PII: S0920-5861(98)00504-5

elevated temperatures under vacuum, or reducing it by either H_2 or CO at moderate temperatures, non-stoichiometric oxides CeO_{2-x} ($0<x<0.5$) are easily obtained [9]. Oxygen vacancies are the predominant atomic point defects responsible for non-stoichiometry in ceria [10], which then appears as a n-type semiconductor [11]. Oxygen vacancies were calculated to be more easily formed at the ceria surface than in the bulk [12]. Upon partial O elimination from O^{2-} in the ceria structure, so forming O-vacancies, the remaining electrons may be a priori either completely delocalised in the conductor band, or distributed among few $Ce^{\delta+}$ cations surrounding the so-created O-vacancy, or localised on Ce^{4+} forming Ce^{3+} [8]. Full discrete localisation of excess electrons into individual Ce^{3+} ions appeared to be a more correct description [8].

Adsorbed probe molecules were used to investigate the properties of ceria surface, assumed as constituted of Ce^{4+} and O^{2-} ions, being more or less co-ordinatively unsaturated as compared to their co-ordination in the bulk. The description is based on the Lewis acid–base concepts, Ce^{4+} being the acidic centre while O^{2-} being the basic one. Molecular probes acting as electron donor, such as CO, pyridine, acetonitrile, dimethyl ether, are currently used for the characterisation of acidic sites on the metal oxides, while the characterisation of basic O^{2-} sites is generally a more troublesome task when their basic strength is high [13]. Using a proton donor such as pyrrole, which was successfully applied in the case of zeolites [14,15], leads to a complete dissociation of pyrrole into pyrrolate ions on O^{2-} sites, indicating a very high basic strength of the sites but not allowing a classification in a base scale through a measurement of the stretching ν(NH) shift [16]. Then halogenated weaker RC–H proton donors (such as chloroform [17] and pentafluorobenzene [18]) were tentatively used in our laboratory. There is, in fact, a lack of basicity probes which encouraged us to investigate the utility of those molecules; but in this case a partial halogenation of the ceria surface by some probe decomposition modified the surface properties themselves. Being negative, these results were never published. On another hand, CO_2 may be used as a Lewis acidic probe [13]. In practical use, even when the surface of a metal oxide got rid from any residual impurities by purification, residual OH species often remains on the surface. Then acid–base properties of adsorbed OH species have to be considered.

The co-ordinative unsaturation of surface cations is characterised by anions resulting from the dissociation of molecular probe upon adsorption. Probes such as adsorbed hydroxy or methoxy species, from water or methanol dissociation, increase the co-ordination of the surface cations as do the structural surface O^{2-} anions. Thus the ν(OH) and ν(OC) stretching modes of hydroxy and methoxy species, respectively, are used to characterise the co-ordinative unsaturation of the surface cationic sites. The relation between the co-ordinative unsaturation of surface cations and the exposed crystallographic planes is far to be obvious. Some calculations described the unsaturation of cations for preferentially exposed crystallographic planes stable at 0 K [7,8], but most of the IR experiments were performed upon divided polycrystalline samples, pre-treated at elevated temperatures for cleaning and then quenched to room temperature for adsorption of the probe. The mobility of the surface oxygen in ceria is strikingly high at 673 K, while the bulk oxygen mobility was already observed between 573 and 723 K; then the morphology of small ceria crystallites in a non-equilibrium thermodynamic state [19] (on which IR probes were adsorbed) is intended to be highly dependent on the pre-treatment, and also possibly on the structure of the precursor salt used to prepare ceria.

Taking out surface capping oxygen upon reduction increases the exposed unsaturation of surface cerium cations, while oxygen vacancies appear in the material structure when oxygen is removed from surface underlayers. IR probes may then be used to study modifications of acid–base properties, as well as oxydoreduction ones, upon reduction.

Although most of the molecular probes are polyfunctional, having both electron donor and electron acceptor centres, they are classified in the paper by looking for what is the main specificity of the probe.

2. Results and discussion

2.1. Background spectra

Ceria powder has been pressed into a disc (ca. 10 mg cm^{-2}), and then submitted to a thermal treat-

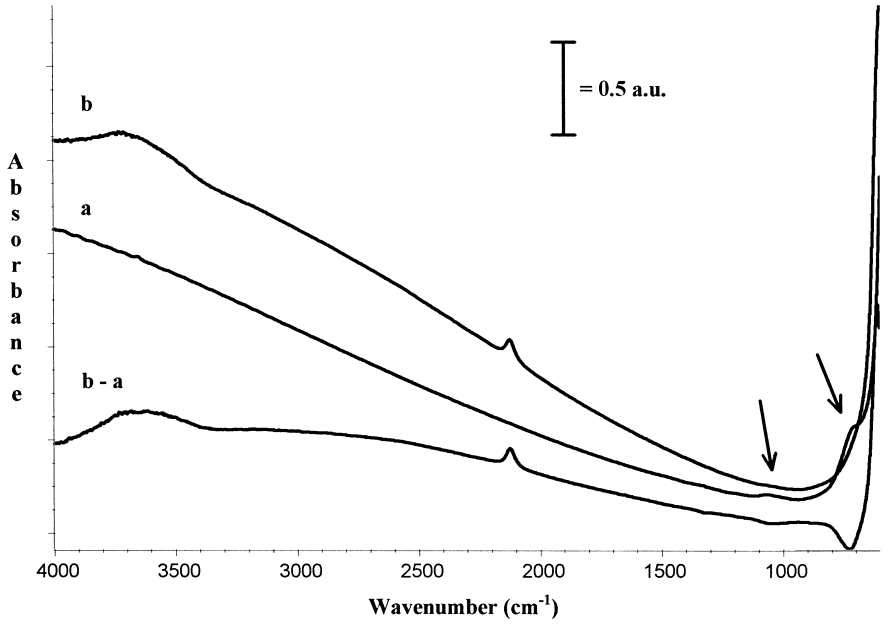

Fig. 1. Background spectra (at r.t.) of pressed ceria powder after O_2 treatment at 1073 K (a) and subsequent reduction by H_2 at 1073 K (b). The (b−a) curve is the corresponding subtraction.

ment under O_2 up to 1073 K. In this treatment all sample contaminants were eliminated. The background spectrum is shown in Fig. 1 (curve a). The optical transparency is good down to 600 cm^{-1}, i.e. above the phonon modes spectral range, but the absorbance increases almost linearly with the frequency. For the sample used here, particle sintering is intended to be observed upon heating above 873 K, increasing so the particle size. Hence, for samples pretreated at temperatures lower than 873 K (instead of 1073 K in Fig. 1), the background absorbance increases more abruptly from 1000 to ca. 3000 cm^{-1}; thereafter, it grows slowly above 3000 cm^{-1}. The apparent loss in transparency in the high wave number range is partly related to light scattering by ceria particles [20]. Some weak features at 1025 and 730 cm^{-1} are indicated with arrows in the spectrum a (Fig. 1). These bands vanish upon H_2 reduction at 1073 K (spectrum b and subtraction b−a) and would be restored upon O_2 re-oxidation at r.t. [21]. Multiphonon processes may be involved to explain such bands [20] as well as surface modes, either a fundamental ν(CeO) mode (730 cm^{-1}) or a first overtone (1025 cm^{-1}) of a fundamental vibration at 530 cm^{-1} [21].

Ceria textural properties may be changed during a reduction process, hence modifying its light scattering properties. Indeed the background profile is more or less reduction treatment dependent, but mainly above 3000 cm^{-1} i.e. in the spectral range where the light scattering factor is found to operate dominantly. Beyond textural properties, electronic ones have to be considered. To minimise the effect of textural properties, the reduction effect may be examined on a sample already sintered by a pre-treatment at 1073 K (Fig. 1). Upon reduction, a well-defined band appears at 2127 cm^{-1}. It was primarily assigned to occluded CO species [22] from carbonate impurities; using well-cleaned samples this assignment was discarded. An electronic origin was also proposed for this band, either an electronic transition from donor levels located near the conduction band such as Ce^{3+} or oxygen vacancies [20] or the forbidden $^2F_{5/2} \rightarrow ^2F_{7/2}$ electronic transition of Ce^{3+} located at subsurface (or bulk) defective lattice sites [21]. An electronic origin was also suggested for the bump observed at around 3700 cm^{-1} (Fig. 1, spectrum b) [21], but it would be different from the previous one since this feature is observed for reduction temperatures higher than 973 K, while the band at 2127 cm^{-1} already appears

when operating the reduction at 673 K. When reducing at temperatures higher than 873 K, a weak and very wide absorption extending from ca. 3500 to 1000 cm^{-1} with a maximum at 2500 cm^{-1} is possibly found (Fig. 1, subtraction b−a) which would be related to semiconductive properties of ceria. In fact, in similar compounds (like ZnO [23]), a broad electronic absorption is observed in this spectral range when bulk defects are created.

Indeed, some intensity attenuation of bands due to adsorbed species was proposed to be related to the presence of electrons delocalised into the ceria conduction band [20]. However, an important effect of the ceria reduction on the intensities of the bands due to adsorbed species may be discarded from the study of the $\nu(CH_3)$ and $\nu(OC)$ bands of methoxy species adsorbed either on unreduced or reduced ceria, at least at room temperature (see below).

2.2. Lewis base properties of ceria

2.2.1. Adsorption of a proton donor: pyrrole

The H-donor pyrrole molecule was reported as a very performing probe to test the O^{2-} basicity of various zeolites [14,15]. The importance of ν(NH) frequency downshift due to the $NH\cdots O^{2-}$ hydrogen bonding interaction is thus used to measure O^{2-} basicity. Spectra due to pyrrole adsorption on ceria [16] either unreduced or H_2 reduced at 673 K are reported in Fig. 2. Spectrum a is simpler and corresponds to a small quantity (ω) of pyrrole adsorbed on reduced ceria. Main features of the spectra are due to the pyrrolate ion, well characterised by the stretching ring modes at 1444 and 1367 cm^{-1} and by the ν(CH) ones at 3100 and 3060 cm^{-1}. Wave numbers for those vibrations in the pyrrolate ion are lower than that for the homologous undissociated pyrrole molecule, i.e. 1533, 1425 cm^{-1} for ring modes and 3136, 3100 cm^{-1} for ν(CH) bands as measured for undissociated pyrrole adsorbed on zeolites [16]. The ν(OH) vibration of the OH species resulting from the pyrrole dissociation is clearly seen at 3628 cm^{-1} only slightly perturbed by the co-adsorbed pyrrolate ions. Almost identical features have been seen for the ring modes when pyrrole was adsorbed on unreduced ceria (Fig. 2, spectrum b); however, in the latter case, the ν(OH) vibration is not interpreted as corresponding to nearly free OH species but to hydrogen bonded ones, partly involving a $OH\cdots PY^-$ interaction (PY^-, pyrrolate anion). In this interaction the ν(CH) vibrations disappear into a complex band structure extending down to 2500 cm^{-1} and for which a coupling between the ν(CH) modes and ring deformations has been proposed [16]. Then ring stretching modes may discern between a dissociative or a non-dissociative adsorption of pyrrole. For ceria the complete dissociation of pyrrole is indicative of the high basicity of surface O^{2-} ions, but this does not allow an investigation of its variation upon reducing ceria.

Non-dissociative weaker H proton donors would be intended to be used as probes. In this purpose, using halogenated hydrocarbons is not very satisfactory

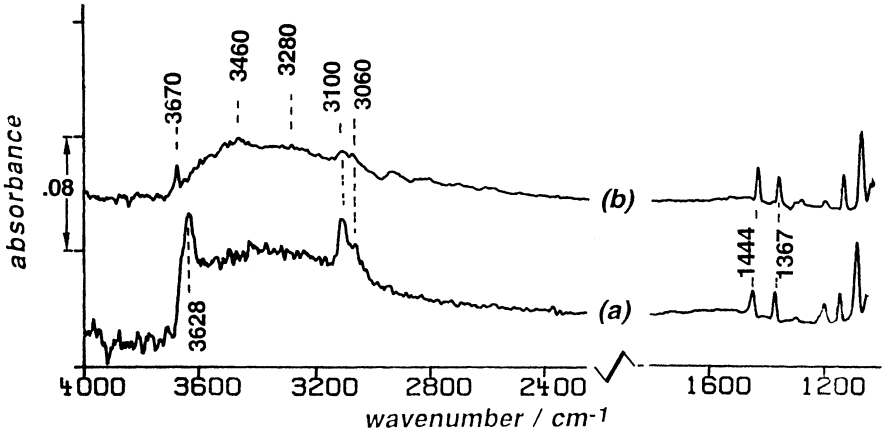

Fig. 2. Adsorption of pyrrole on ceria either reduced (a) or unreduced (b); ω=35 μmol g^{-1}.

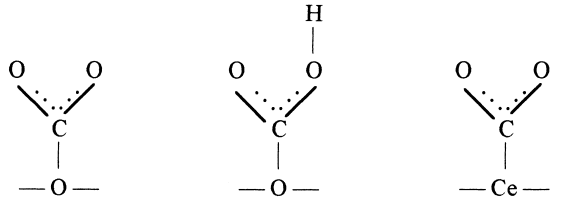

Scheme 1.

because of the occurrence of surface halogenation. The rather inert methane molecule was adsorbed on ceria at low temperature (173 K) [24]. The symmetry loss of CH_4 upon adsorption modifies the infrared activity of the $\nu(CH_4)$ modes. From this result, the presence of two types of surface O^{2-} ions was proposed.

2.2.2. *Adsorption of an electron acceptor: CO_2*

CO_2 may act as a Lewis acid toward either O^{2-} surface ions (so forming carbonate species) or residual basic OH surface species, hydrogen carbonates so being produced. The formation of carboxylate species was also considered. The above-mentioned compounds are described in Scheme 1. As far as adsorbed carbonate species are concerned, their principal anchoring structures are shown in Scheme 2 in the commonly accepted representation. In this scheme the polydentate carbonate oxygen atoms interact with cerium cations, but precise geometry for this interaction cannot be made.

Spectral characterisation of species from CO_2 adsorption is very useful for the detection of surface impurities, CO_2 being an unavoidable atmospheric contaminant for ceria. Moreover, when ceria is obtained using cerium carbonate or other organic compounds as precursors, carbonates are the residual species after thermal decomposition of the cake. Beyond a general characterisation of carbonate, hydrogen carbonate, carboxylate species over various oxides [25], such compounds have been more specifically studied when adsorbed on ceria [20,26–28]. As CO_2 (1.3 kPa) is introduced at room temperature (r.t.) on ceria O_2 pre-treated and outgassed at 873 K (Fig. 3, spectrum a), the resulting spectrum is in agreement with literature data [26,28]. Note that the adsorption at r.t. is not instantaneous [26]: a delay of ca. 10 min is needed to reach a near equilibrium state. The different adsorbed species may be discerned by outgassing the sample and then heating it under vacuum (Fig. 3, spectra b–f); their characteristic bands are reported in Table 1.

Two hydrogen carbonate species I and II were discerned. Species I vanishes upon evacuation at r.t., while heating at 373 K is needed to eliminate species II. The two different compounds may result from CO_2 interaction with OH groups either mono- or bicoordinated with cerium surface cations. Bands due to bridged carbonates are very weak and these species desorb upon evacuation at r.t.; it was proposed that bands at 1219 and 1396 cm^{-1} could be assigned to bridged carbonates [26], but they were in fact due to traces of hydrogen carbonates. In another connection, we cannot completely discard the alternative assignment of the bridged species bands to CO_2 molecularly adsorbed in a bent form [29]. Bidentate carbonates are well-characterised species. Contrarily, the band assignment to mono- and polydentate carbonates in Table 1 is far to be obvious.

The formation of the so-called polydentate carbonates from CO_2 adsorption implies more than a displacement of O^{2-} ions and also that of Ce^{4+}, i.e. a

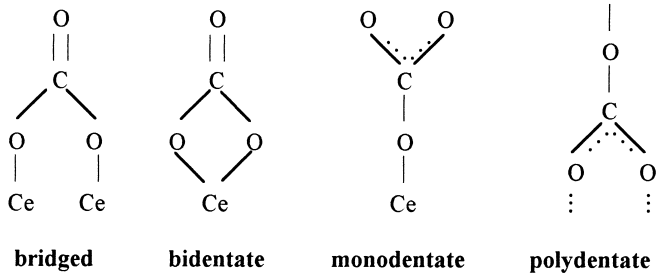

Scheme 2.

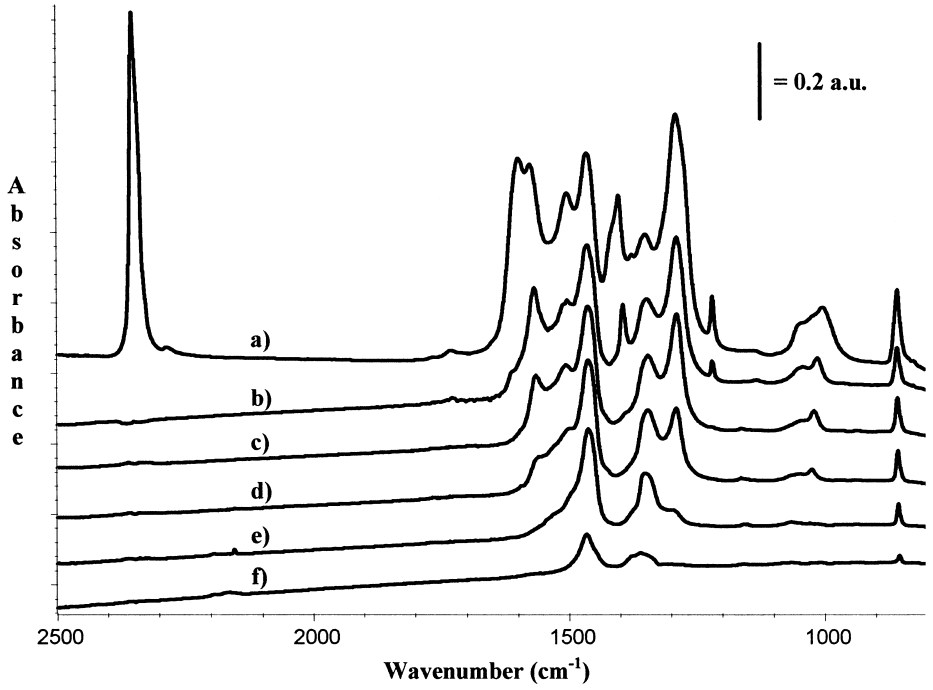

Fig. 3. Adsorption of CO_2 at r.t. (a) on activated ceria and after evacuation at r.t. (b), 373 K (c), 423 K (d), 473 K (e) and 573 K (f).

Table 1
Adsorbed species from CO_2 adsorption on unreduced ceria at r.t.: wave numbers (cm^{-1}) for their characteristic bands

Species	$\nu(CO_3)$	$\pi(CO_3)$	δ(OH)	ν(OH)
Hydrogen carbonates				
(I)	1599, 1413, 1025	823	1218	3617
(II)	1613, 1391, 1045	836	1218	3617
Carbonates				
Bridged	1736, 1135, –	–		
Bidentate	1567, 1289, 1014	856		
Monodentate[a]	1504, 1351, –	–		
Polydentate[b]	1462, 1353[c], 1066	854		

[a]Only the high wave number band is easily identified in spectra; it was as well assigned to carboxylate species [26] (see text).
[b]These bands were alternatively assigned to monodentate species (see text).
[c]When only weak amounts of polydentate carbonates remain on the surface, several bands may be found between 1395 and 1350 cm^{-1}.

surface reorganisation. A structure similar to that of bulk carbonates is thought to be hence reached. Three features support the above assignment to polydentate species:

1. the wave numbers are very close to those reported for bands due to anhydrous cerium carbonate $Ce(CO_3)_2$ [30];
2. the corresponding bands are the only ones which are observed during the cleaning treatment of ceria produced via cerium carbonate;
3. the high thermal stability of the species is explainable by their bulk-like structure [25].

Only the high wave number band (1504 cm^{-1}) assigned to a monodentate carbonate in Table 1 is

generally clearly identified in experimental spectra. It was found to be accompanied by a very weak band at 1310 cm^{-1} and assigned to carboxylate species [26] on the basis of similar features observed for inorganic carboxylates. However, the formation of the reduced CO_2^{2-} form of CO_2 would need a ceria re-oxidation, hence the presence of some reduced centres on the surface [28,31]. In our opinion, outgassing a ceria sample at moderate temperatures cannot create sufficient amount of defects to explain the relative intense band at 1504 cm^{-1}. So we have performed CO_2 adsorption on a ceria sample prepared from cerium nitrate and pre-treated under O_2 at 873 K, then reduced under H_2 at the same temperature to eliminate nitrite impurities, and finally re-oxidised by O_2 at 873 K and cooled down under O_2 to room temperature. This was followed by a brief evacuation at r.t. just before CO_2 adsorption; any ceria reduction after this experimental treatment is discarded. Fortunately, in that conditions, bands due to polydentate carbonates were sufficiently weak to allow the clear observation of two bands at 1504 and 1351 cm^{-1}, that simultaneously vanish after a prolonged evacuation at r.t. Thus, in Table 1, we have proposed the attribution of these bands to monodentate carbonates rather than to carboxylate species.

Adding $^{13}CO_2$ instead of $^{12}CO_2$ produces similar isotopic shifts for the higher wave number bands of carbonate species: 1736→1691 cm^{-1} (bridged), 1567→1530 cm^{-1} (bidentate), 1504→1465 cm^{-1} (monodentate) and 1462→1425 cm^{-1} (polydentate), and hence a same isotopic ratio near 1.026 is obtained. This reinforces (but does not prove) the assignment of these bands to similar species (carbonates).

Considering the attribution made in Table 1, the species desorb in the following increasing temperature order upon outgassing: hydrogen carbonates, bridged carbonates (r.t.)<bidentate carbonates (423 K)<monodentate carbonates (473 K)<polydentate carbonates (573 K and above).

When CO_2 was adsorbed at r.t. on ceria H_2 reduced at 823 K, mainly bidentate carbonate species were observed but with the high wave number $\nu(CO_3)$ band located at 1586 cm^{-1} instead of 1565 cm^{-1} for unreduced ceria [28]; ill-defined mono- and polydentate species were also observed. Upon heating, the $\nu(CO_3)$ band located at 1586 cm^{-1} shifts to 1567 cm^{-1} inferring the ceria re-oxidation. Conversely, when CO was adsorbed on unreduced ceria, bidentate carbonate species were mainly observed at r.t. [26], but upon heating polydentate species become predominant assessing the CO ceria reduction through bulk-like carbonate species formation.

2.3. Lewis acid properties

2.3.1. Adsorption of CO

Crudely, CO acts as a σ-electron donor through the 5σ orbital mainly localised on C atom and as a π acceptor through the antibonding $2\pi^*$ orbital, the last property being important only when interacting with cations having incomplete d-shell. Using the 2143 cm^{-1} value for the ν(CO) mode in gaseous CO as a reference, the extent of the upward shift of this vibration wave number is commonly used to evaluate the acidity of the cationic adsorption site when CO interacts as a Lewis base towards a non-d-electron cation.

When adsorbing CO at r.t. on unreduced ceria generally two ν(CO) bands are observed with wave numbers depending on the materials: 2177, 2156 cm^{-1} [26], either 2165, 2150 cm^{-1} [20] or 2170, 2151 cm^{-1} [28]. As CO is adsorbed at r.t., carbonate species immediately produced may induce some electronic effects at the cationic adsorption sites. To give an example of an induced effect, chlorination (which prevents carbonate species formation) induces a band shift up to 2187 cm^{-1} [32]. To avoid surface carbonation, CO has to be introduced at low temperatures. Spectra are shown in Fig. 4 for CO adsorbed at 77 K on unreduced ceria; they are coverage dependent. At high CO coverage a band at 2151 cm^{-1} is largely predominant with, on its both sides, a band at 2162 cm^{-1} and a shoulder at 2140 cm^{-1} (spectrum a). Upon evacuation the more loosely held CO species desorb first, thus presenting two consequences: (i) the relative importance of high wave number bands increases, and (ii) the wave numbers are upward shifted because of the decrease of the effect of intermolecular interaction on their values. Thus (spectrum b) the band at 2140 cm^{-1} vanishes upon evacuation, while bands at 2151 and 2162 cm^{-1} are shifted to 2157 and 2168 cm^{-1}, the relative importance of the band at 2157 cm^{-1} being decreased. The 2168 cm^{-1} value is in accordance with literature results [33,34]. The two bands observed at 2168 and 2157 cm^{-1} could

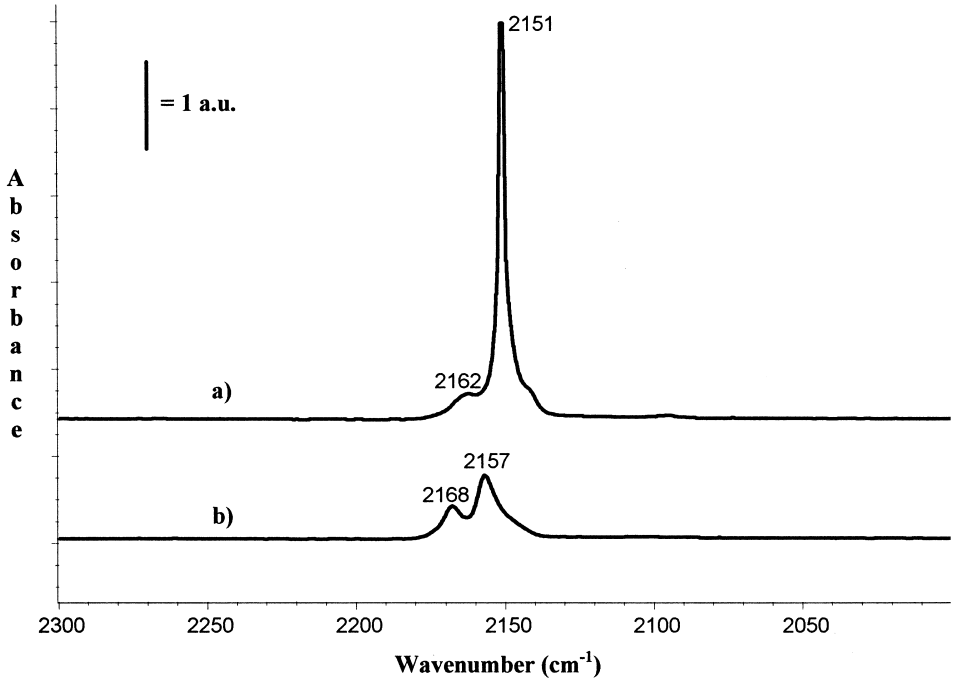

Fig. 4. Adsorption of CO (13.3 kPa) at 77 K on activated ceria (a) and after evacuation (10^{-2} Pa) (b).

be assignable to CO adsorbed on Ce^{4+} cations with different unsaturated co-ordination [20,26]. The 2157 cm^{-1} was also assigned to defects associated with Ce^{3+} [35]. However, recalling that a ν(CO) band at 2152 cm^{-1} may be found for CO hydrogen bonded with not very acidic surface OH species (as in alumina [36,37]), such an assignment may also be considered in the case of ceria. Indeed, a somewhat ill-defined downshift of the ν(OH) bands is observed as CO is adsorbed. Taking into account for van der Waals interactions either between CO molecules or between CO molecules and surface, and specific Lewis interaction between CO and co-ordinatively unsaturated Ce^{4+} surface sites, bands at 2140, 2157 and 2168 cm^{-1} may be assigned as follows. The band at 2140 cm^{-1} is found whatever the oxide on which CO is adsorbed and it is then ascribed to liquid-like CO (tridimensional phase). The band at 2157 cm^{-1}, shifted not very upward from unperturbed CO in gas phase (2143 cm^{-1}), is assignable to physisorbed CO weakly interacting with the surface (bidimensional phase), the interaction including both van der Waals forces and weak CO interaction with surface OH species. The band at 2168 cm^{-1} is attributed to CO co-ordinated with Ce^{4+} cations and its shift from the gas phase value (2143 cm^{-1}) is a measure of the Lewis acid strength. The following acidity order for oxides has then been established: $MgO<CeO_2<TiO_2$ [34]. Notice that when CO was adsorbed at r.t. on very small ceria particles supported on silica, a ν(CO) band was observed at 2180 cm^{-1} [38]. This high value was ascribed to a high co-ordinative unsaturation of Ce^{4+} ions [38].

As CO was adsorbed on reduced ceria a band at 2126 cm^{-1} was proposed to be due to the $Ce^{3+}\cdots CO$ interaction [20,35]. Such a band was not observed when adsorbing CO at low temperature on reduced ceria, but another one could be located at 2161 cm^{-1} [33]. Taking the 2143 cm^{-1} value for CO in the gas phase as origin, the shift (18 cm^{-1}) lower than that (26 cm^{-1}) due to the $Ce^{4+}\cdots CO$ interaction shows that the Lewis acidity of the cerium cation decreases when reduced. Similarly, the ν(CO) band shifts from 2187 to 2172 cm^{-1} upon Ce^{4+}/Ce^{3+} reduction of chlorinated ceria [32]. Beyond the above molecular adsorption, chemisorbed species are found to be formed when CO is adsorbed at r.t. on H_2 reduced ceria. Crudely, for reduction temperature below

873 K, formate species are mainly produced [27,28], but for higher reduction temperatures carbonites CO_2^{2-} species are found to be formed [39].

Note that similar to CO, carbon dioxide may act as a σ-donor. Thus the linear adsorption of CO_2 on cationic sites shifts upward the ν_3 asymmetric stretching mode from its 2349 cm^{-1} value in the gas phase. It was suggested that the shift depends on the Lewis acid site strength [29]. Such a ν_3 band is clearly seen at 2353 cm^{-1} when CO_2 was adsorbed on unreduced ceria (Fig. 3); the same value was found for reduced ceria thus excluding any reduction effect. The ν_1 symmetric mode was discerned as a weak and narrow band at 1377 cm^{-1}.

2.3.2. *Adsorption of pyridine*

Pyridine acts as a strong Lewis base through the electronic lone pair of its N atom and is currently used as a probe for Lewis or Brønsted acidities [40–42]. It may be preferred to CO when weak surface acidities are concerned. Ring vibrational mode frequencies are more or less shifted by the interaction of pyridine with surface Lewis acid centres, the 8a mode being more sensitive. The 8a mode is located at 1580 cm^{-1} for liquid-like (van der Waals) physically adsorbed pyridine [41] and is shifted upward by pyridine adsorption on Lewis centres. When adsorbed on ceria at r.t. (Fig. 5), only bands due to molecularly adsorbed pyridine are observed [43,44], but pyridine cracking occurred upon heating above 100°C [43]. The 8a mode was observed mainly at 1595 cm^{-1} either for unreduced [43,44] or reduced ceria [44]. Another weak band at 1623 cm^{-1} was also assigned to the 8a mode for pyridine adsorbed on more acidic centres [43], but it is more likely due to the (1+6a) combination mode [45]. Thus, no effect of ceria reduction on cationic acidity appears from pyridine adsorption.

The 15 cm^{-1} upward shift of the 8a wave number upon pyridine adsorption may be compared to the shifts observed when adsorbed on ZrO_2 (27 cm^{-1}) or on TiO_2 (30 cm^{-1}) [46]. This infers that the Lewis acidity of ceria is lower than that of ZrO_2 and TiO_2.

2.3.3. *Adsorption of dimethylether (DME) and acetonitrile*

Similar to CO and pyridine, DME and acetonitrile are Lewis bases because of the O and N atoms electronic lone pair. They are scarcely used as probes

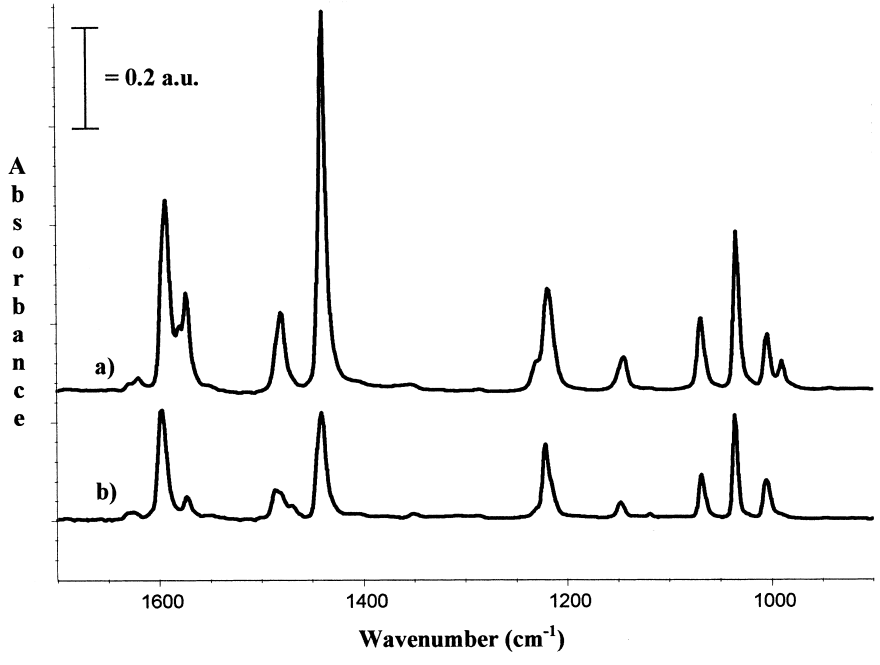

Fig. 5. Adsorption of pyridine (1.3×10^2 Pa) at r.t. on activated ceria (a) and after evacuation (10^{-2} Pa) at r.t. (b).

for the study of the surface acidity of metal oxides. Then the interest of such probes is a priori rather limited as far as the comparison of the relative acidity of the surface of various oxides is needed. So the adsorptions of such probes are only briefly mentioned in this paper.

Adsorption of DME on unreduced ceria at r.t. is non-dissociative and three intense bands at 1156, 1076 and 912 cm^{-1} are observed in the ν(COC) spectral range [47]. The bands at 1156 and 1076 cm^{-1} are due to a coupling between a rocking CH_3 mode and the asymmetric stretching ν_a(COC), while the band at 912 cm^{-1} is the symmetric ν_s(COC) vibration. When compared to the corresponding wave number values for DME in a carbon tetrachloride solution, the downward shifts of 20 or 10 cm^{-1} for the asymmetric and symmetric ν(COC) modes are similar to the shifts due to the hydrogen bonding HCl–DME interaction [48]. Then the Lewis acidity of ceria is rather low and similar to the acidity of a proton donor. No significant differences between spectra of DME adsorbed on ceria either unreduced or reduced [47] were observed indicating so a similar weak Lewis acid strength.

The adsorption of acetonitrile on ceria, either reduced or not, is rather complex [49] because of the high basicity of ceria. Acetonitrile dissociates on surface O^{2-} ions forming the CH_2CN^- mono-anion or reacts producing the acetamide di-anion. For CH_3CN adsorbed at r.t. on unreduced ceria three ν(CN) bands at 2251, 2258 and 2269 cm^{-1} are ascribed, respectively, to liquid-like CH_3CN, physisorbed molecules bound to ceria via van der Waals forces and CH_3CN specifically adsorbed on Lewis sites [49]. For comparison, the ν(C≡N) band is located at 2254 cm^{-1} for pure liquid being, for example, shifted to 2268 cm^{-1} when CH_3CN is hydrogen bonded to trifluoroethanol in solution [50]. Then a very similar upward ν(CN) shift for CH_3CN interacting either with ceria Lewis centres or through H-bonding is observed. This confirms that the Lewis acidity of unreduced ceria is weak and similar to the acidity of a proton donor having a mid strength. No molecularly adsorbed CH_3CN species were observed at r.t. in the case of reduced ceria. Hence it appears that CO and CH_3CN probes are able to discern between the acidities of unreduced and reduced ceria, but not pyridine or DME. This would not only be related to the relative basic strength of the probes but also, possibly, to some specific behaviour due to the presence of π orbitals of (C≡N) and (C≡O) groups.

2.4. Redox properties of ceria and co-ordinatively unsaturated (CUS) surface ions

Substoichiometric CeO_{2-x} ceria is produced upon O elimination from CeO_2 and the subsequent O vacancies formation. The complete re-oxidation by O_2 is easy even at r.t. and may proceed following the general scheme [51]:

$$O_{2\,g} \rightarrow O_{2\,ads} \rightarrow O^-_{2\,ads} \rightarrow O^{2-}_{2\,ads} \rightarrow 2O^-_{ads} \rightarrow 2O^{2-}_{lc}$$

where O^{2-}_{lc} is a lattice oxygen ion. However, for ceria, superoxide O^-_2 and peroxide O^{2-}_2 species are characterised by IR technique only when the reduction is very limited as surface defects.

2.4.1. Reduced surface defects: superoxide and peroxide species

Reduced surface defects on ceria surface may be created upon heating under vacuum already at a temperature as low as 473 K. These defects could result from residual surface species decomposition such as hydroxy and carbonate species as impurities [31] or from some lattice O^{2-} species easily removable from the surface (in that case a thermal treatment at higher temperatures is thought to be needed). Adsorbing O_2 on such pre-treated samples (or on samples pre-treated by H_2 below 420 K [52]) produces superoxide O^-_2 species well characterised by their O–O vibration at 1126 cm^{-1} [20,31,53] and its overtone at 2237 cm^{-1} [54]. Superoxide species are not stable upon outgassing at r.t. or upon heating at mild temperatures (373 K) under O_2 pressure [31,55]. Only on partially H_2 reduced ceria, peroxide O^{2-}_2 species are observed being characterised by their vibration at 883 cm^{-1} [52].

2.4.2. Lattice reduction: characterisation of surface cationic sites

H_2 reduction of ceria through H_2O elimination was found to begin at 473 K. In the case of low-surface-area sample a surface reduction step was observed between 573 and 623 K, not easy discernible from underlayers reduction in the case of high surface area samples. In any case, a $CeO_{1.83}$ stoichiometry is reached before ceria is further reduced at temperatures

higher than 923 K [22]. Although ceria has a surface and bulk oxygen mobility strikingly high [19], its reduction at mild temperatures may be governed by kinetic rather than thermodynamic considerations. In the range 573–773 K the surface reduction process is faster than the O diffusion from the bulk to the surface [56]. Consequently, in most of the IR studies of ceria reduction using surface probes at r.t., the results depend upon (i) the reaching of the dynamic state according to the pre-treatment temperature, and (ii) the more or less complete quenching of the surface state on cooling down to room temperature. Not too highly reduced ceria is re-oxidised by O_2 even at r.t. [57,58].

As far as H_2 is used as a reducing agent, the reduction of cerium ions occurs not only through H_2O elimination but also through the reversible H_2 adsorption/desorption process [59].

Tetracyanoethylene (TCNE) was used as an electron acceptor for characterisation of metal oxide by electron paramagnetic resonance [60,61]. Adsorbing TCNE under its vapour pressure at r.t. on unreduced ceria mainly produces the tricyanoethenolate anion in relation to the presence of highly basic centres [62]. On the contrary $TCNE^{x-}$ (x=1, 2, 3) anions were found to be produced when TCNE was adsorbed on ceria reduced at 823 K. The $TCNE^{x-}$ anions were characterised by their ν(CN) bands at 2196, 2184, and 2174 cm^{-1} ($TCNE^{-}$), 2161, 2120, and 2098 cm^{-1} ($TCNE^{2-}$), and 2053 and 2004 cm^{-1} ($TCNE^{3-}$). The formation of such species infers a high electron donor strength of reduced ceria. The presence of three anions does not imply three distinct reduced sites but is rather due to a multilayered adsorption of TCNE [62].

To characterise specifically the cationic sites, anionic adsorbed species are more appropriate than neutral probes. Adsorbed hydroxy species and the parent methoxy ones are thus very useful as they may complete the co-ordination sphere of surface cations. In the ceria lattice, O^{2-} ions are tetrahedrically co-ordinated to four Ce^{4+} cations. Then, looking the cationic site as a local truncation of the bulk, three types of adsorbed hydroxy (or methoxy) species are intended to be observed [63] as described in Scheme 3.

Hydroxy species are denoted as I, II or III according to the number of cerium cations constituting the adsorption site.

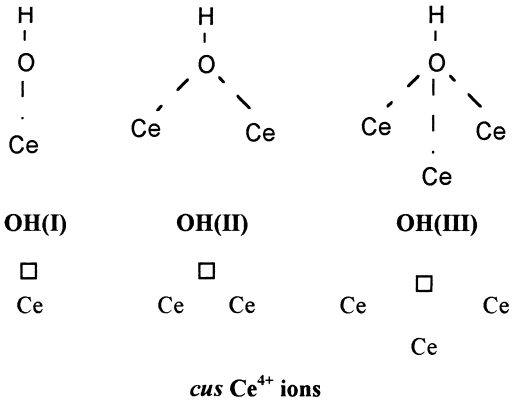

Scheme 3.

2.4.3. Hydroxy species

Surface hydroxy species would be produced by H_2O dissociation on Ce^{4+} O^{2-} sites of ceria through the breaking of one of the HO–H bond so forming two adsorbed OH species. However, we have to have in mind that when adsorbed on reduced ceria, H_2O may re-oxidise ceria with H_2 evolution. Although the re-oxidation of ceria by H_2O was studied at mild temperatures (ca. 573 K [64]), it was already observed at r.t. for highly reduced samples [65]. On the other hand, at high coverage hydrogen bonding between OH surface species themselves or water produces broad stretching ν(OH···) bands preventing the characterisation of the surface by free OH species described in Scheme 3. Then free OH groups are usually observed as residual species after the application of a partial deshydroxylation (or deshydratation) treatment to the sample. Being residual species, they are not necessarily representative of the overall cationic sites on the surface. In our opinion, the use of the methoxy surface probe (see below) instead of the hydroxy one should circumvent the above-mentioned difficulties.

Spectra in Fig. 6 show results coherent with H_2 dissociation at 573 K on ceria and not with H_2O dissociation. The sample was first cleaned under O_2 at 873 K; in such a way that no residual OH species are observed after the pre-treatment (spectrum a). After 0.5 h of treatment under 13 kPa of H_2 at 573 K and cooling down to r.t. under H_2, the resulting spectrum (b) is very similar to that obtained exposing unreduced ceria to water vapour [66], indicating that H_2 has not reduced ceria appreciably. The OH species of Scheme

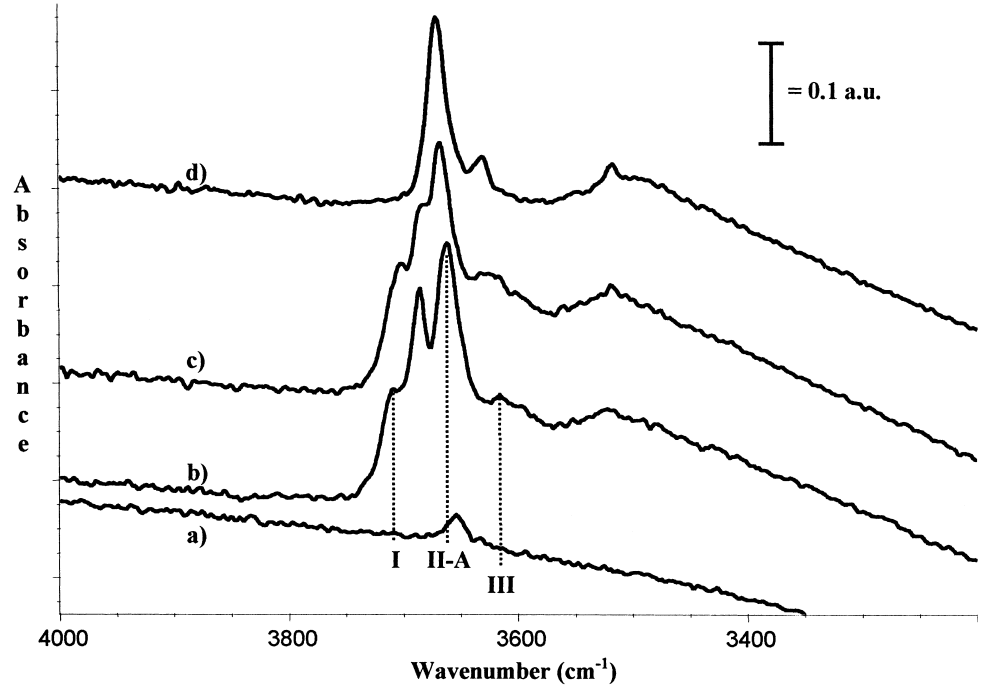

Fig. 6. ν(OH) bands for a ceria sample after activation (a), first introduction of 13 kPa of H_2 for 0.5 h (b), second introduction of 13 kPa of H_2 for 0.5 h (c) and third introduction of 13 kPa of H_2 for 0.5 h (d) at 573 K.

3 are then characterised by the ν(OH) bands at 3710 (I), 3660 (II-A) and ca. 3600 (III) cm^{-1} (the notation II-A is used here because other type II species may be observed) [66]. The ν(OH) band at 3686 cm^{-1}, a broad ν(OH$\cdots$) band at ca. 3300 cm^{-1} and a very weak δ(HOH) bending at 1630–1595 cm^{-1} were assigned to undissociated water molecules. A ν(OH) band may be seen at 3510 cm^{-1} and attributed to oxyhydroxy species [66], or possibly to hydroxy carbonates if residual carbonates remain in the sample [67]. Only after the third introduction of H_2, OH bands due to OH(I) and water species disappear (spectrum d), indicating so a beginning of reduction.

When ceria has been submitted to three successive H_2 exposures (0.5 h each) separated by an evacuation step, the spectra of residual OH species after quenching to r.t. (Fig. 7) are dependent on the temperature of treatment. Neither OH(I) species nor undissociated water adsorbed molecules are observed for $T_r \geq 573$ K, but the relative importance of the band at 3651 cm^{-1} (denoted II-B) increases till T_r=773 K, accompanied by a broad $\nu(OH_b)$ band at ca. 3400 cm^{-1} due to hydrogen bonded OH species. This was assigned to a surface–subsurface reorganisation [66]. Simultaneously, the ν[OH(II-A)] wave number increases (Table 2) in relation with ceria reduction by H_2O elimination. At 873 K, the ν[OH(II-A)] band becomes predominant at 3660 cm^{-1}, again indicating a transient re-oxidation of the surface caused by O migration from the bulk and subsequent bulk reduction.

Beyond the effect of ceria surface reduction through oxygen elimination, the ν(OH) (II-A, B) wave numbers are also slightly dependent on H coverage in relation, possibly, to the so-called "reversible" ceria reduction [59]. Indeed, when reducing ceria at 773 K, the spectrum at r.t. under 13 kPa of H_2 (Fig. 8(a)) shows: the ν[OH(II-A)] band at 3683 cm^{-1}, the ν[OH(II-B)] one at 3655 cm^{-1} and the $\nu(OH_b)$ at ca. 3400 cm^{-1}. After outgassing at 773 K (spectrum b), H-bonded OH species have disappeared and the remaining II-B are characterised by a weak band shifted from 3655 to 3640 cm^{-1}; the ν[OH(II-A)] is nearly unchanged being only shifted from 3683 to 3680 cm^{-1}. After a new exposure

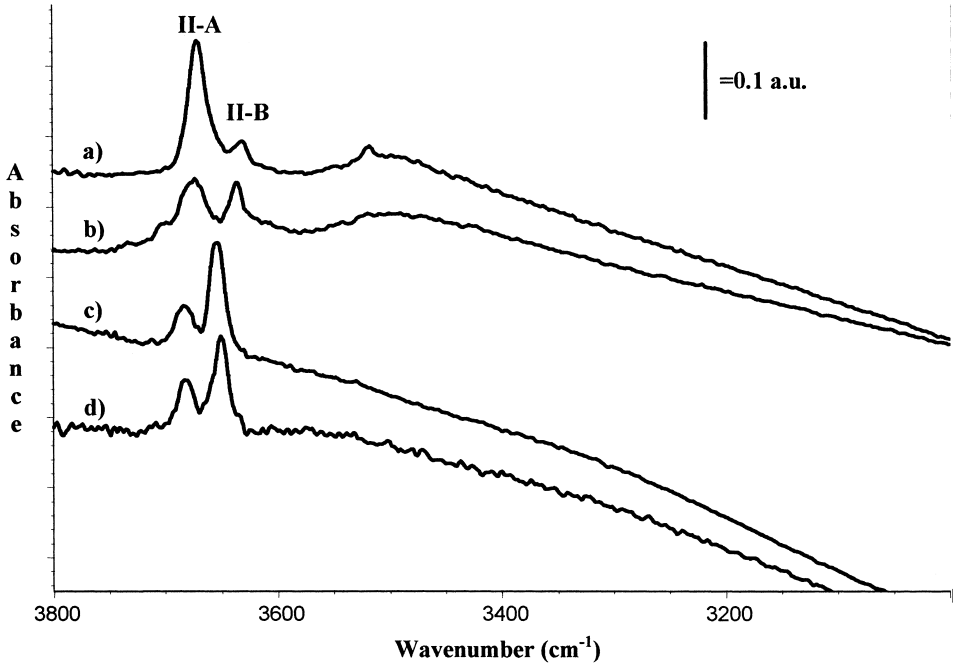

Fig. 7. ν(OH) bands for ceria samples treated three times under H_2 (13 kPa) for 0.5 h at 573 K (a), 623 K (b), 673 K (c) and 773 K (d).

Table 2
ν(OH) and ν(OC) wave numbers (cm^{-1}) for OH and OCH_3 species adsorbed at r.t. on ceria after 3×0.5 h pre-exposure of the sample to H_2 at the indicated temperature T_r (except at 573† where the ν(OH) value was obtained after only 1×0.5 h exposure to H_2 avoiding appreciable reduction)

T_r (K)	573†	573	623	673	773
OH(II-A)	3662	3671	3673	3681	3683
OCH_3(II-A)	–	1062	1072	1078	1081

For residual OH species, values are those observed under 13 kPa H_2.

of the sample to 13 kPa of H_2 at 773 K (spectrum c), the initial spectrum (a) is restored inferring the reversibility of the process during hydrogen adsorption/desorption.

In conclusion, the OH probe on the ceria surface indicates the presence of mainly type I and II cationic sites (Scheme 3). Type I sites are not present on reduced surface while OH(II-A) and (II-B) species are sensitive to the surface reduction either through oxygen elimination or by H_2 reversible adsorption. The surface state observed at r.t. appears as a quenching of the state obtained during the pre-treatment at higher temperatures.

2.4.4. Methoxy species

Methanol dissociates into methoxy groups when adsorbed at r.t. Using $CH_3^{18}OH$, it was found that the so-formed methoxy species result from the O–H (not the C–O) bond breaking [68]. Attention has to be drawn to the fact that surface chlorination of ceria prevents the methanol dissociation [69]. Moreover, CO_2 from not tightly bound carbonate species as impurities may react with methoxy species producing methyl carbonates. On a high surface area ceria sample calcinated in O_2 at 673 K, the methoxy coverage was 4.2 $OCH_3\,nm^{-2}$, i.e. near a monolayer [70]; however, in other experiments in our laboratory using

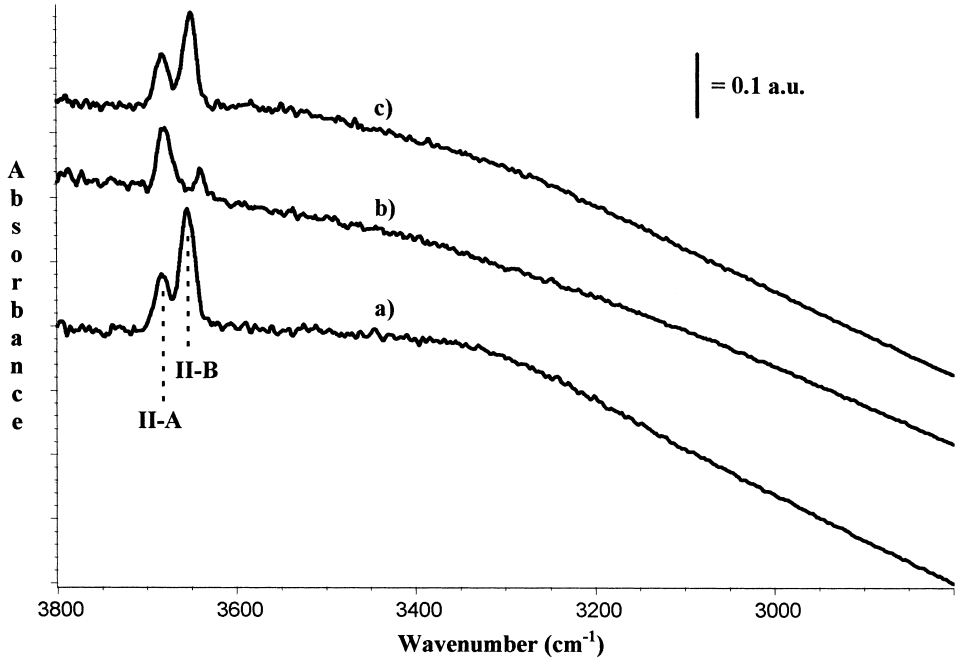

Fig. 8. ν(OH) bands for a ceria sample treated under H_2 (13 kPa) for 0.5 h at 773 K (a), evacuated at about 10^{-2} Pa at the same temperature (b) and submitted again to 13 kPa of H_2 for 0.5 h at 773 K (c).

a ceria sample pre-treated at 873 K, a lower value (2.8 OCH_3 nm^{-2}) was obtained. Whatever be the result, the OCH_3 surface coverage is high and the species probes the whole surface.

The spectrum a in Fig. 9 corresponds to the ν(O–C) vibration of methoxy species adsorbed on ceria pre-exposed to H_2 at 573 K; it is similar to the spectrum arising from methanol adsorption on unreduced ceria [70]. Similar to OH groups on unreduced ceria, three methoxy species are clearly characterised by the bands at 1106 (I), 1062 (II-A) and 1015 cm^{-1} (III). As in the case of the OH(III) species, the band due to OCH_3(III) species is weak. A shoulder is clearly seen at 1042 cm^{-1} on the low frequency side of the ν[OC(II-A)] band and it is assigned to a denoted OCH_3(II′) species. Note that the ν(OC) band for the II′ species and the ν(OH) one for the II-B ones are similarly located between bands due to II-A and III species, but beyond this there are no proofs that the cationic sites for II′ and II-B species are similar, so a distinct notation is used here.

As surface oxygen vacancies are produced by surface reduction at 623 K, the co-ordinative unsaturation of cationic sites increases, and the intensity of the ν[OC(I)] band decreases (Fig. 9, spectrum b). The wave number for the ν[OC(II-A)] band increases as did the ν[OH(II-A)] band (the same II-A notation for the two bands is based upon their similar behaviour upon reduction: see Table 2). When the ν[OC(I)] band vanishes almost completely after H_2 reduction at 673 K, shifting from 1106 up to 1112 cm^{-1} (spectrum c), a new band ν[OC(II^*)] is seen at 1083 cm^{-1} on the high frequency side of that assigned to the ν[OC(II-A)] stretching. Here, the II^* notation is used for that band instead of II-B [69,70] to avoid a misleading similarity with the ones denoted as OH(II-B). It was shown that I sites are converted into II^* ones [70] upon surface reduction; as OH(I) species disappear in this reduction process, no residual equivalent OH(II^*) species are intended to be found on the surface. For ceria reduced at 773 K (Fig. 9, spectrum d) ν[OC(II^*)] and ν[OC(II-A)] bands are confused possibly through a surface–subsurface reorganisation of the sample.

Then two cationic I and II-A surface sites are mainly observed on unreduced ceria either from methoxy species or from residual OH groups. As the sur-

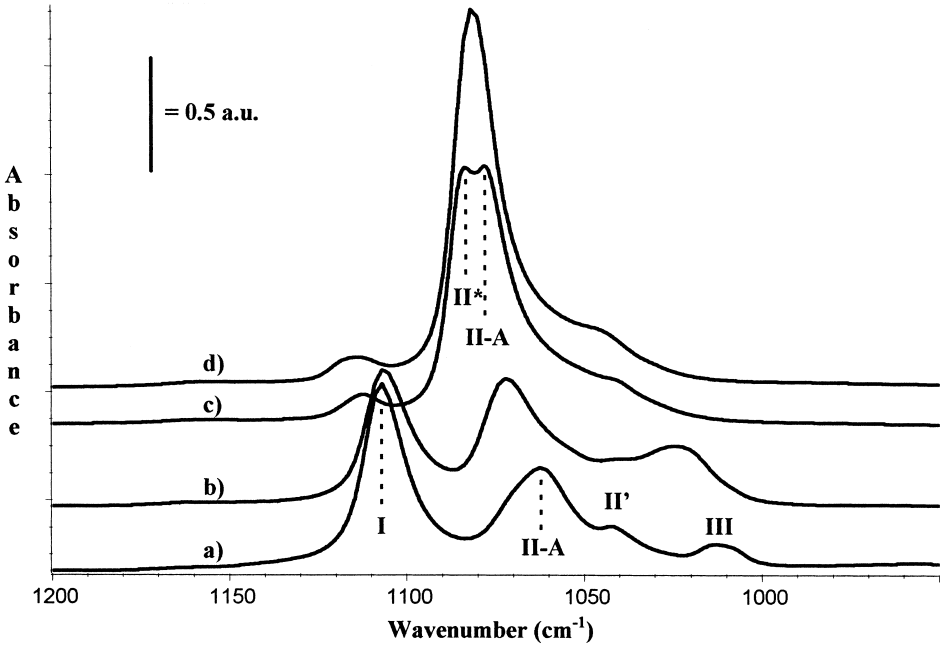

Fig. 9. ν(OC) bands for methoxy groups on ceria reduced by H_2 at 573 K (a), 623 K (b), 673 K (c) and 773 K (d).

face reduction degree increases, the wave numbers for both the ν[OH(II-A)] and ν[OC(II-A)] bands also increase (Table 2). Using OCH_3 species as probes, the surface reduction is easily studied by the conversion of species OCH_3(I) into OCH_3(II*).

The I→II* site conversion upon reduction is reversed by O_2 addition at r.t., at least for ceria reduced by H_2 below 773 K. Spectra obtained by adding successive doses of O_2 from the initial spectrum of methoxy species adsorbed on ceria reduced at 673 K are shown in Fig. 10, illustrating the II*→I site conversion. For ceria reduced at temperatures higher than 773 K, bulk reduction is more important and the local thermal effect due to the re-oxidation by oxygen is thought to induce some re-oxidation of the surface methoxy probe. For ceria reduced by H_2 below 773 K, the II*→I site conversion upon re-oxidation may be used to measure the oxygen storage capacity (OSC) of the sample adding known amounts of O_2 [70]. When the reduction is not too deeply extended into the bulk, a correlation is observed between the OSC and the ν[OC(II-A)] wave number for methoxy species adsorbed on ceria sample initially reduced at various temperatures (Fig. 11).

In the νCH_3 spectral range of methoxy species vibrational modes, the band for the symmetric $\nu_s(CH_3)$ mode is well defined. It is observed at 2803 cm^{-1} for OCH_3 species and it is shifted downwards to 2782 cm^{-1} upon ceria reduction [70]; note that direction of the shift is opposite with respect to that observed for the ν[OC(II-A)] band (Table 2). But whereas the ν(OC) band wave number depends upon both the co-ordinative unsaturation of the cationic site (a geometrical factor) and the electronic state of cerium ions, the $\nu_s(CH_3)$ wave number depends mainly on the oxidation state of cerium ions alone, being $\nu_s(CH_3)$ band due to OCH_3(I) species unresolved with respect to those due to OCH_3(II) species [70].

2.4.5. *Formate species*

Wave numbers of bands due to adsorbed formates $HCOO^-$ depend upon the reduction state of ceria surface as well as features due to other ionic adsorbed species such as carbonates. Spectra of formates are complementary to that mentioned here owing to the occurrence of adsorbed formate species in widely studied processes such as CO and H_2 reaction or

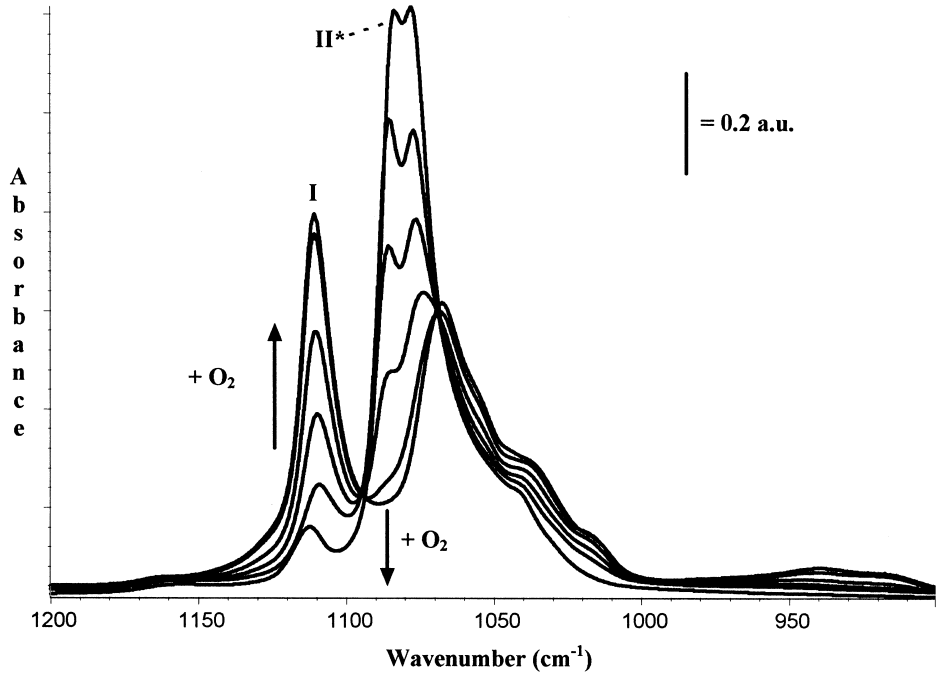

Fig. 10. Spectra of methoxy groups on a ceria sample reduced by H_2 at 673 K and progressively re-oxidised by O_2 at r.t.

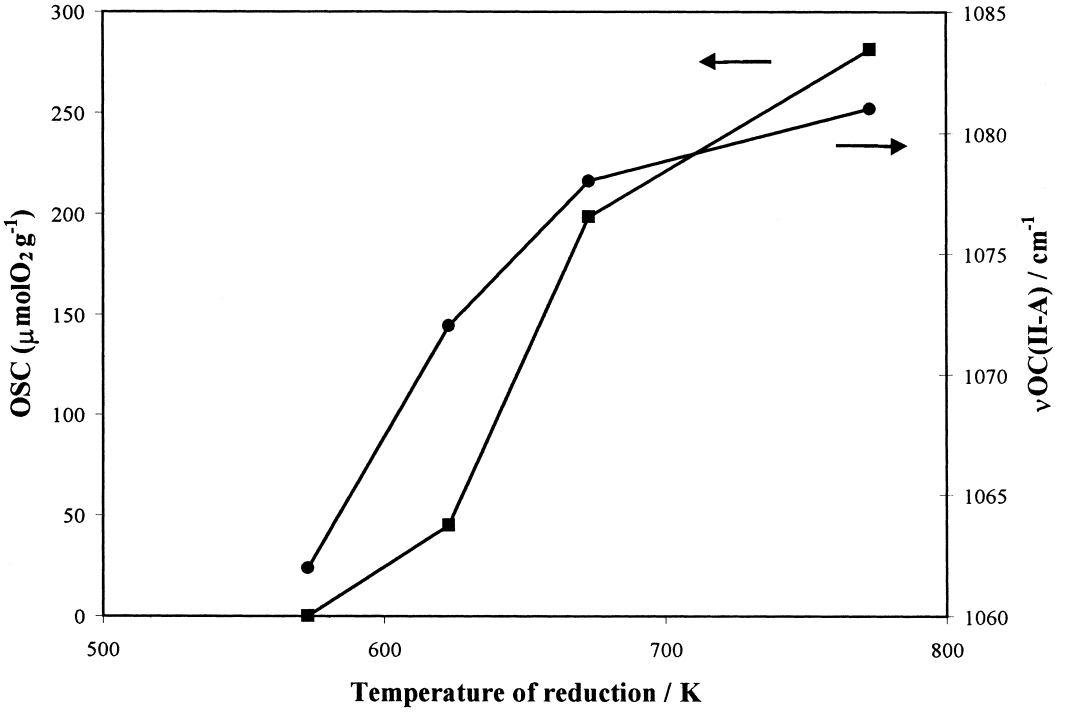

Fig. 11. Trend of the ν[OC(II-A)] wave number and OSC vs. reduction temperature for ceria samples.

CO adsorption on reduced metals supported on ceria. Vibrational modes of adsorbed formate species are clearly identified by adsorbing formic acid on unreduced ceria: ν(C–H), 2845; ν_{as}(OCO) 1599, 1553, 1542; δ(CH), 1371; ν_s(OCO) 1362, 1248; and δ(OCO) 777 cm^{-1} [71]. Minor bands appear also at 2933 and 2723 cm^{-1} and are assigned, respectively, to the combination δ(C–H)+ν_s(OCO) and to the overtone 2δ(C–H). The ν_{as}(OCO) and ν_s(OCO) bands at 1599 and 1248 cm^{-1} were assigned to monodentate formate species, and the others being assigned to bidentate ones [71]. Bands due to monodentate formates are scarcely reported and remain not precisely defined, being proposed to be located at 1620 and 1300 cm^{-1} from formaldehyde adsorption [71].

Isotopic $^{16}O \rightarrow ^{18}O$ and H→D substitutions may discern between two bidentate formate species from CO adsorption on H_2 reduced ceria. They are characterised by their ν_{as} and $\nu_s(^{16}OC^{16}O)$ band pairs at either 1577 and 1353 cm^{-1} or at 1587 and 1362 cm^{-1}; the corresponding pairs of bands for bidentate formates on unreduced ceria are at 1552 and 1357 cm^{-1} [28]. For example, the ν_{as} and ν_s(OCO) spectral range is shown in Fig. 12: in the case of curve (d) formates are produced from the selective oxidation of OCH_3(I) species by unreduced ceria upon heating at 473 K. On partially reduced ceria from OCH_3 oxidation into formate, two main ν_{as}(OCO) bands are located at 1550 and 1562 cm^{-1} with a shoulder at 1580 cm^{-1} corresponding to bidentate formate species on unreduced (1550 cm^{-1}) or reduced (1562 and 1580 cm^{-1}) cerium sites. As formate species are produced here through ceria reduction, the fact that they are not necessarily observed on reduced sites is in accordance with their high surface mobility [28], which may involve transient HCO formyl species. The simultaneous presence of formyl and formate species was proposed during the reaction of adsorbed CO to formates on reduced ceria, assigning two weak bands at 2796 and 2706 cm^{-1} to the ν(CH) mode of formyl species [27].

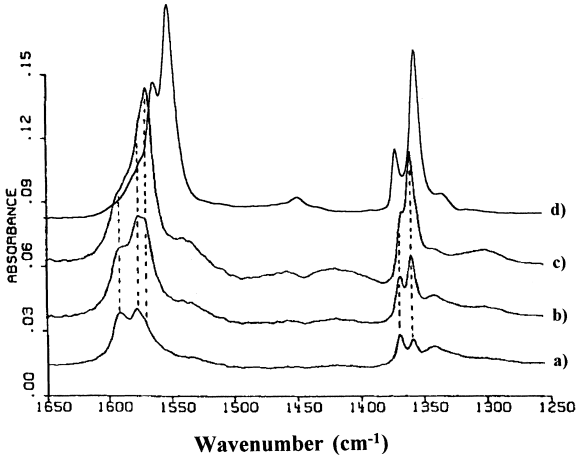

Fig. 12. Spectra of formate species evolution vs. time after CO introduction at r.t. on a ceria sample reduced by H_2 at 823 K, at t=0 (a), t=5 min (b) and t=15 min (c); spectra of formate species after methanol introduction at r.t. on a ceria sample then heated at 473 K (d).

3. Conclusion

FT-IR spectroscopy appears as a useful tool for surface characterisation of ceria. Care has to be taken to the presence of electronic transition features in the infrared spectral range when reducing the sample. The weak but well-defined band at 2127 cm^{-1} (assignable to the electronic transition of Ce^{3+} ions in bulk defective sites) is indicative of a reduced state. The Lewis basicity of ceria reduced or not appears to be quite high, but probes are not able to quantify the strength. By contrast, the Lewis acidity is weak and comparable to that of a proton donor giving rise to a hydrogen bond of mid strength. The high oxygen mobility of ceria may explain the formation of reduced surface defect sites upon mild reducing treatment; superoxide species are so transiently produced when oxygen is adsorbed on such sites at r.t. or below. As surface hydroxy or methoxy species complete the coordination sphere of surface cations, they are good probes to study their co-ordinative unsaturation and reduction state. For samples reduced by H_2 at different temperatures, using OH species as probes, it may be shown that (i) the reduction begins at 573 K, (ii) a surface/subsurface reorganisation takes place at ca. 773 K, and (iii) a surface re-oxidation from O-bulk migration is observed at 873 K. Then the surface state observed quenching the sample to r.t. is strictly dependent on the pre-treatment. Quantitatively, the oxygen storage capacity of reduced ceria may be measured by oxygen volumetric introductions using methoxy species spectra as indicative of the reduction state.

However, the method is limited to samples not too deeply reduced because of thermal effects in the ceria re-oxidation process, allowing the oxidation of the methoxy probe itself.

References

[1] A. Trovarelli, Catal. Rev. Sci. Eng. 38 (1996) 439 and references therein.
[2] A. Fujimori, Phys. Rev. B 28 (1983) 2281.
[3] A. Kotani, H. Mizuta, T. Jo, J.C. Parlebas, Solid State Commun. 53 (1985) 805.
[4] E. Wuilloud, B. Delley, W.D. Schneider, Y. Baer, Phys. Rev. Lett. 53 (1984) 202.
[5] D. Koelling, A. Boring, J. Wood, Solid State Commun. 47 (1983) 227.
[6] S. Hill, C.R.A. Catlow, J. Phys. Chem. Solids 54 (1993) 411.
[7] T. Sayle, S. Parker, C.R.A. Catlow, Surf. Sci. 316 (1994) 329.
[8] J. Conesa, Surf. Sci. 339 (1995) 337.
[9] R. Körner, M. Ricken, J. Nölting, I. Riess, J. Solid State Chem. 78 (1989) 136.
[10] J. Faber, M. Seitz, M. Mueller, J. Phys. Chem. Solids 37 (1976) 909.
[11] J. Herrmann, E. Ramaroson, J. Tempere, M. Guilleux, Appl. Catal. 53 (1989) 117.
[12] T. Sayle, S. Parker, R.C.A. Catlow, J. Chem. Soc., Chem. Commun. (1992) 977.
[13] J.C. Lavalley, Catal. Today 27 (1996) 377.
[14] D. Barthomeuf, J. Phys. Chem. 88 (1984) 42.
[15] M. Huang, S. Kaliaguine, J. Chem. Soc., Faraday Trans. 88 (1992) 751.
[16] C. Binet, A. Jadi, J. Lamotte, J.C. Lavalley, J. Chem. Soc., Faraday Trans. 92 (1996) 123.
[17] F.M. Slasinski, J.M. Tustin, F.J. Sweeney, A.M. Armstrong, Q.A. Ahmed, J.P. Lorand, J. Org. Chem. 41 (1976) 2693.
[18] J.R. Murdoch, A. Streitwieser Jr., , J. Phys. Chem. 85 (1981) 3352.
[19] D. Martin, D. Duprez, J. Phys. Chem. 100 (1996) 9429.
[20] F. Bozon-Verduraz, A. Bensalem, J. Chem. Soc., Faraday Trans. 90 (1994) 653.
[21] C. Binet, A. Badri, J.C. Lavalley, J. Phys. Chem. 98 (1994) 6392.
[22] A. Laachir, V. Perrichon, A. Badri, J. Lamotte, E. Catherine, J.C. Lavalley, J. El Fallah, L. Hilaire, F. le Normand, E. Quéméré, G.N. Sauvion, O. Touret, J. Chem. Soc., Faraday Trans. 87 (1991) 1601.
[23] F. Boccuzzi, G. Ghiotti, A. Chiorino, J. Chem. Soc., Faraday Trans. 2 79 (1983) 1779.
[24] C. Li, Q. Xin, J. Phys. Chem. 96 (1992) 7714.
[25] G. Busca, V. Lorenzelli, Mater. Chem. 7 (1982) 89.
[26] C. Li, Y. Sakata, T. Arai, K. Domen, K.I. Maruya, T. Onishi, J. Chem. Soc., Faraday Trans. I 85 (1989) 929.
[27] C. Li, Y. Sakata, T. Arai, K. Domen, K.I. Maruya, T. Onishi, J. Chem. Soc., Faraday Trans. I 85 (1989) 1451.
[28] C. Binet, A. Jadi, J.C. Lavalley, J. Chim. Phys. Phys. Chim. Biol. 89 (1992) 1779.
[29] G. Ramis, G. Busca, V. Lorenzelli, Mater. Chem. Phys. 29 (1991) 425.
[30] J. Goldsmith, S. Ross, Spectrochim. Acta A 23 (1967) 1909.
[31] J. Soria, A. Martinez-Arias, J. Conesa, J. Chem. Soc., Faraday Trans. 91 (1995) 1669.
[32] A. Badri, C. Binet, J.C. Lavalley, J. Phys. Chem. 100 (1996) 8363.
[33] A. Badri, C. Binet, J.C. Lavalley, J. Chem. Soc., Faraday Trans. 92 (1996) 1603.
[34] M. Zaki, H. Knözinger, Spectrochim. Acta A 43 (1987) 1455.
[35] M. Zaki, B. Vielhaber, H. Knözinger, J. Phys. Chem. 90 (1986) 3176.
[36] M. Zaki, H. Knözinger, Mater. Chem. Phys. 17 (1987) 201.
[37] F. Maugé, J.C. Lavalley, J. Catal. 137 (1992) 69.
[38] A. Bensalem, F. Bozon-Verduraz, M. Delamar, G. Bugli, Appl. Catal. A 121 (1995) 81.
[39] C. Binet, A. Badri, M. Boutonnet-Kizling, J.C. Lavalley, J. Chem. Soc., Faraday Trans. 90 (1994) 1023.
[40] T. Barzetti, E. Selli, D. Moscotti, L. Forni, J. Chem. Soc., Faraday Trans. 92 (1996) 1401.
[41] C. Morterra, G. Cerrato, Langmuir 6 (1990) 1810.
[42] J. Lercher, C. Gründling, G. Eder-Mirth, Catal. Today 27 (1996) 353.
[43] M. Zaki, G. Hussein, S. Mansour, H. El-Ammawy, J. Mol. Catal. 51 (1989) 209.
[44] A. Jadi, Ph.D. Thesis, University of Caen, France, 1990.
[45] C. Morterra, G. Magnacca, J. Chem. Soc., Faraday Trans. 92 (1996) 5111.
[46] C. Lahousse, A. Aboulayt, F. Maugé, J. Bachelier, J.C. Lavalley, J. Mol. Catal. 84 (1993) 283.
[47] C. Binet, J.C. Lavalley, J. Phys. Chem. B 101 (1997) 1484.
[48] J. Le Calvé, P. Grange, J. Lascombe, C.R. Acad. Sci. (Paris) 261 (1965) 2075.
[49] A. Jadi, C. Binet, J.C. Lavalley, J. Chim. Phys. Phys. Chim. Biol. 89 (1992) 31.
[50] G. Eaton, A. Pena-Nunez, M. Symons, J. Chem. Soc., Faraday Trans. I 84 (1988) 2181.
[51] M. Che, A.J. Tench, Adv. Catal. 31 (1982) 77.
[52] C. Li, K. Domen, K.-I. Maruya, T. Onishi, J. Am. Chem. Soc. 111 (1989) 7683.
[53] J. Soria, J. Coronado, J. Conesa, J. Chem. Soc., Faraday Trans. 92 (1996) 1619.
[54] C. Li, K. Domen, K.-I. Maruya, T. Onishi, J. Chem. Soc., Chem. Commun. (1988) 1541.
[55] X. Zhang, K. Klabunde, Inorg. Chem. 31 (1992) 1706.
[56] J. El Fallah, S. Boujana, H. Dexpert, A. Kiennemann, J. Majerus, O. Touret, F. Villain, F. le Normand, J. Phys. Chem. 98 (1994) 5522.
[57] V. Perrichon, A. Laachir, G. Bergeret, R. Fréty, L. Tournayan, O. Touret, J. Chem. Soc., Faraday Trans. 90 (1994) 773.
[58] S. Bernal, J. Calvino, G. Cifredo, J. Gatica, J. Pérez Omil, J. Pintado, J. Chem. Soc., Faraday Trans. 89 (1993) 3499.
[59] S. Bernal, J. Calvino, G. Cifredo, J. Rodriguez-Izquierdo, J. Phys. Chem. 99 (1995) 11794.

[60] B. Flockhart, I. Leith, R. Pink, Trans. Faraday Soc. 65 (1969) 542.
[61] M. Che, C. Naccache, B. Imelik, J. Catal. 24 (1972) 328.
[62] C. Binet, A. Jadi, J.C. Lavalley, J. Chim. Phys. Phys. Chim. Biol. 88 (1991) 449.
[63] A. Tsyganenko, V. Filimonov, J. Mol. Struct. 19 (1973) 579.
[64] K. Otsuka, M. Hatano, A. Morikaya, J. Catal. 79 (1983) 493.
[65] C. Padeste, N. Cant, D. Trimm, Catal. Lett. 18 (1993) 305.
[66] A. Badri, C. Binet, J.C. Lavalley, J. Chem. Soc., Faraday Trans. 92 (1996) 4669.
[67] S. Bernal, F. Botana, R. Garcia, J. Rodriguez-Izquierdo, React. Solids 4 (1987) 23.
[68] J. Lamotte, V. Morávek, M. Bensitel, J.C. Lavalley, React. Kinet. Catal. Lett. 36 (1988) 113.
[69] A. Badri, C. Binet, J.C. Lavalley, J. Chem. Soc., Faraday Trans. 93 (1997) 2121.
[70] A. Badri, C. Binet, J.C. Lavalley, J. Chem. Soc., Faraday Trans. 93 (1997) 1159.
[71] C. Li, K. Domen, K.-I. Maruya, T. Onishi, J. Catal. 125 (1990) 445.